Turkish Journal of Electrical Engineering & Computer Sciences

http://journals.tubitak.gov.tr/elektrik/

Research Article

Turk J Elec Eng & Comp Sci
(2017) 25: 1059 – 1069

doi:10.3906/elk-1511-115

On the application of the spectral element method in electromagnetic problems involving domain decomposition

Ibrahim MAHARIQ*
Department of Electrical and Electronics Engineering, University of Turkish Aeronautical Association, Ankara, Turkey

Received: 13.11.2015 • **Accepted/Published Online:** 19.03.2016 • **Final Version:** 10.04.2017

Abstract: One of the challenges in electromagnetics is to solve electromagnetic fields originated from a radiating source or a scattering object in distances that largely exceed the dimensions of the source or scatterer. In this paper, domain decomposition based on the application reasoning of the perfectly matched layer (PML) is studied by the spectral element method (SEM) for the first time in order to solve near and far electromagnetic fields without requiring substantially computational resources. Scattering from a loss-free dielectric cylinder and radiated fields from a line source are the problems utilized for the purpose of numerical demonstration in two dimensions in order to verify the successful application of SEM and its accuracy under domain decomposition. It is demonstrated that it is possible to accurately solve for near-field and far-field zones where millions of unknowns are encountered by using a typical personal computer.

Key words: Domain truncation, electromagnetic fields, numerical methods, radiation, scattering

1. Introduction

Until the 1940s, most of electromagnetic problems that involve simplicity were solved by analytical methods [1], mainly by separation of variables and integral equation methods. In addition, a lot of effort was given to extend the application of these methods to a narrow range of practical problems. However, complexity in geometries associated with the most realistic problems was the main reason behind developing numerical methods that can easily be performed by computing machines [2].

The most common numerical methods used in electromagnetic modeling are [2,3] the finite-difference time-domain method (FDTD), method of weighted residuals, method of moments, finite element method (FEM), and Monte Carlo method. Generally speaking, computational methods in the numerical modeling of electromagnetic scattering and radiation problems are based either on the direct discretization of the governing partial differential equations or on the discretization of the integral equations that reformulate the associated boundary value problems [4].

Recent years have seen a lot of progress in our capability to simulate and design very complex electromagnetic systems [3]. Still, there are some challenges in the modeling of electromagnetic problems. One of these challenges is the limitations in computational resources. That is, in numerical modelling, the approximation to Maxwell's equations returns a large system of linear equations to be solved by a computer. The resulting system of equations sometimes exceeds the limit of the available computational resources. To overcome

*Correspondence: ibmahariq@gmail.com

this problem, the multilevel fast multipole algorithm (MLFMA) was introduced to accurately solve large-scale scattering problems [5–7].

For the purpose of reducing the burden computationally, as most of electromagnetic problems are unbounded in nature, the well-known technique by which truncation can be successfully applied is the so-called artificial boundary conditions (ABCs). ABCs are essentially based on a differential operator (boundary operator) such as the Trefethen–Halpern general ABC and Higdon boundary operator [8]. Yet, the electromagnetic community were not relatively satisfied by ABCs for two main reasons. First, ABCs have to be placed at a distance away from the region of interest, and this placement adds a computational burden. The second is in terms of accuracy as truncation introduces artificial reflections that deteriorate the solution accuracy [4,9,10]. Berenger [9] changed the way of thinking and introduced the perfectly matched layer (PML), which is superior to the ABCs. Mahariq et al. [11] demonstrated that one can achieve the same accuracy when the PML is utilized for domain truncation (and when it is not for problems whose exact solutions are available) to solve the scattered field from a perfect electric conducting cylinder, where the exact solution is imposed on the outer boundary instead of PML truncation. In addition, PML can be placed much closer to the region of interest than ABCs without deteriorating the accuracy [9–11], and hence reducing the size of the resulting system matrix.

However, in some engineering problems, very important information can be lost when the PML truncation is carried out in the close vicinity of a scatterer or a radiator. In other words, the interest of an engineer sometimes lies in fields that are relatively far away from the source. In such cases, as mentioned earlier, if the domain truncation is performed far away from the source, the corresponding system matrix will dramatically get larger and hence exceed the available computer memory [12]. A very typical example is the interest in solving the near and far fields of radiating antennas. Alternatively, several techniques were applied to transform near-zone FDTD results to far-field zones [13–21].

The current study applies SEM and verifies its accuracy using a domain decomposition technique based on the mathematical reasoning of PML to directly find near and far electromagnetic fields in free space where billions of unknowns can be involved without requiring substantial computational resources (mainly, memory). That is, the novelty of the current study is, first, the adoption of the PML formulation presented by [4] for proposing a domain decomposition technique, and, second, its verification by SEM for the first time. Due to its high accuracy, the spectral element method (SEM) is utilized in order to numerically demonstrate the technique through spatial discretization of the governing partial differential equations in the frequency domain.

2. Verification in 1D

Considering the following 1D problem:

$$\frac{d^2u}{dx^2} + k^2u = 0, \quad \Omega = [x_0, x_n], \quad \text{with} \quad u(x_0) = u_0, \tag{1}$$

One cannot solve such a problem as it is a second-order equation with only one boundary condition being provided. This is a very typical situation where the importance of the perfectly match layer (PML) can be realized. Here $u(x)$ is the function to be solved and $k = 2\pi$. The introduction of PML requires an additional differential equation governing the domain $[x_n, x_b]$ [11]:

$$\frac{1}{a^2}\frac{d^2u}{dx^2} + k^2u = 0, \quad x \in [x_n, x_b], \tag{2}$$

in which

$$a = 1 + \frac{\alpha}{jk}, \tag{3}$$

with α being a real constant number. Here, since the value of α determines the rate at which $u(x)$ is attenuated within the PML, it is called the attenuation factor. As seen from Figure 1, the function $u(x)$ is immediately forced to zero (i.e. $u(x_b) \simeq 0$); hence, the original problem in (1) is turned into a typical boundary value problem as both boundaries are now known. It is important to note that the additional interface conditions between Ω and Ω_{PML} must be satisfied [11].

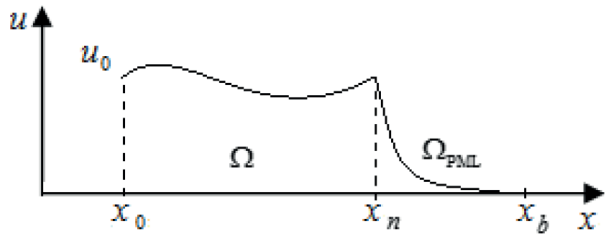

Figure 1. Domain truncation by PML in a 1D problem.

Let us further assume that the region of interest (Ω) is too large for the available computational resources. Then one can subdivide Ω into n adjacent domains as follows:

$$\begin{aligned} \Omega &= \Omega_1 \cup \Omega_2 \cup \Omega_3 ... \cup \Omega_n, \text{ with} \\ \Omega_1 &= [x_0, x_1],\ \Omega_2 = [x_1, x_2], \\ \Omega_i &= [x_{i-1}, x_i], ..., \Omega_n = [x_{n-1}, x_n], \text{ and } \Omega_i \cap \Omega_{i+1} = \Phi, \end{aligned} \tag{4}$$

where $i = 1, 2, 3, \ ... \ n$ and Φ is the null space. By this view, the original problem stated in (1) is partitioned into n-computationally independent problems each of which is governed by the differential equation in (1) and the solution in Ω is obtained as follows:

Step-1: Solve:

$$\begin{aligned} &\tfrac{d^2u}{dx^2} + k^2u = 0, \quad x \in \Omega_1 \\ &\tfrac{1}{a^2}\tfrac{d^2u}{dx^2} + k^2u = 0, \quad x \in [x_1, x_1 + b], \\ &\text{with } u(x_0) = u_0, \text{ and } u(x_1 + b) = 0. \end{aligned} \tag{5}$$

Step-2: Store the solution obtained from step-1 over the domain Ω_1, clear the memory, and then solve the differential equations in (5) over:

$$\begin{aligned} &x \in \Omega_2, \text{ and } x \in [x_2, x_2 + b], \\ &\text{with } u(x_1) = u_1, \text{ and } u(x_2 + b) = 0. \\ &\qquad\qquad\qquad\qquad\qquad\qquad \vdots \end{aligned} \tag{6}$$

Step-n: Store the solution obtained from step-(n-1) over the domain Ω_{n-1}, clear the memory, and then solve the differential equations in (5) over:

$$\begin{aligned} &x \in \Omega_n, \text{ and } x \in [x_n, x_n + b], \\ &\text{with } u(x_{n-1}) = u_{n-1}, \text{ and } u(x_n + b) = 0, \end{aligned} \tag{7}$$

where b stands for the thickness of Ω_{PML}. Attention should be given to the fact that the boundary $u(x_i) = u_i$ which is required to solve over Ω_{i+1} is borrowed from the solution in Ω_i. By applying these steps, one can solve a problem whose domain is extremely large. The previous steps are applied to solve the problem stated in (1) by the spectral element method (SEM). In fact, one can choose x_0 and x_n so that the following exact solution is obtained: $u(x) = \exp(-jkx)$, which is a combination of sine and cosine functions with a period of $\lambda = 1$ and it is chosen to be the length of each subdomain Ω_i. The length of the domain Ω (region of interest) is chosen as: $x_n - x_0 = 500000\lambda$ (hence, $n = 500000$), and in each subdomain the function is represented by 17 nodes as this number is sufficient to resolve one wavelength by SEM. In Figure 2 the maximum relative error (Err) in each subdomain is presented versus x, where Err is defined as follows:

$$Err = \max_i \frac{|u_{i,exact} - u_{i,SEM}|}{|u_{i,exact}|}, \tag{8}$$

in which $u_{i,exact}$ and $u_{i,SEM}$ denote the exact and the SEM solution, respectively, at the ith node. As can be seen from the figure, the error is very slowly increasing although the region of interest is very large in terms of the period length. It took 1.8 h for a computer of 2.3 GHz CPU, while a small percentage of the available memory was utilized over the solution time.

If this problem is solved directly without using the domain decomposition technique presented in the current study, the total number of unknowns will be 500000×17, which is around 9 million, and the size of the system matrix would be around 9×9 million (sparsity is ignored). Therefore, this requires very large memory. Applying this solution technique in two dimensions (2D) is slightly different from the case of 1D as the adjacent subdomains share nonhomogeneous boundaries. Corresponding details are presented in the next section.

3. Two dimensions

The schematic of a typical unbounded 2D electromagnetic scattering where the PML is applied for domain truncation is shown in Figure 3. The PML formulation presented by [4] is utilized in the current study. The authors showed that the following equations governing the PML regions (with its possible realizations; the split-field formulation [9], the anisotropic realization [22], and the bianisotropic realization [23]) can be derived:

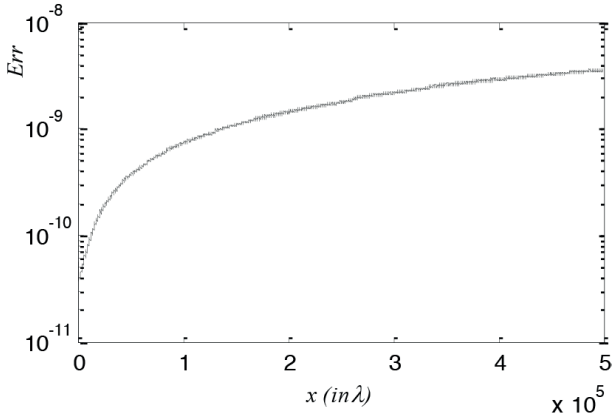

Figure 2. The maximum relative error vs x over the domain Ω.

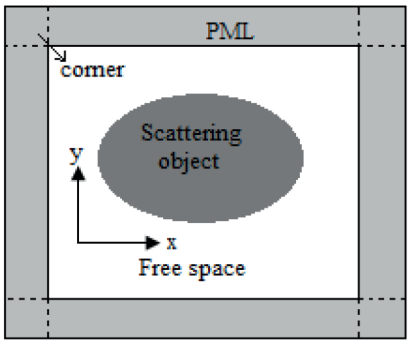

Figure 3. A typical 2D electromagnetic scattering problem truncated by PML.

$$\frac{1}{a}\frac{\partial^2 u}{\partial x^2} + a\frac{\partial^2 u}{\partial y^2} + ak^2 u = 0, \tag{9}$$

$$a\frac{\partial^2 u}{\partial x^2} + \frac{1}{a}\frac{\partial^2 u}{\partial y^2} + ak^2 u = 0, \tag{10}$$

$$\frac{\partial^2 u}{\partial x^2} + \frac{\partial^2 u}{\partial y^2} + a^2 k^2 u = 0, \tag{11}$$

where k is the wavenumber, $u(x,y)$ is a function denoting the plane wave to be solved (with suppressed time dependence $\exp(jwt)$), i.e. $u(x,y)$ stands for $E_z(x,y)$ in TE mode or $H_z(x,y)$ in TM mode, and the homogeneous Dirichlet boundary condition $u = 0$ is set on the exterior boundaries of the PML region. Eq. (9) must be satisfied in x-decay in the PML region, whereas (10) and (11) must be satisfied in y-decay and xy-decay (corner) in the PML, respectively.

The following 2D equations must be satisfied in free space and in dielectric objects, respectively:

$$\frac{\partial^2 u}{\partial x^2} + \frac{\partial^2 u}{\partial y^2} + k^2 u = 0, \text{ and } \nabla.(\frac{1}{\mu_r}\nabla u) + k^2 \varepsilon_r u = k^2(1-\varepsilon_r)u^{inc}, \tag{12}$$

where μ_r and ε_r stand for relative permeability and relative permittivity, respectively, and u^{inc} is the incident field. As mentioned earlier, in some cases the interest lies in finding the near and far electromagnetic fields around the scatterer or the radiator. However, the limitations in the computational resources restrict us to truncate the free space in the close vicinity of sources or scattering objects, and hence losing the details about the solution in farther distances becomes a problem.

Therefore, by extending the proposed technique introduced for 1D to 2D, the solution over Ω can be obtained as follows: assume that the available memory can be utilized at most in solving the field over Ω_{11}, which is a subset of Ω and includes the sources (see Figure 4), with Ω being partitioned into equal subdomains:

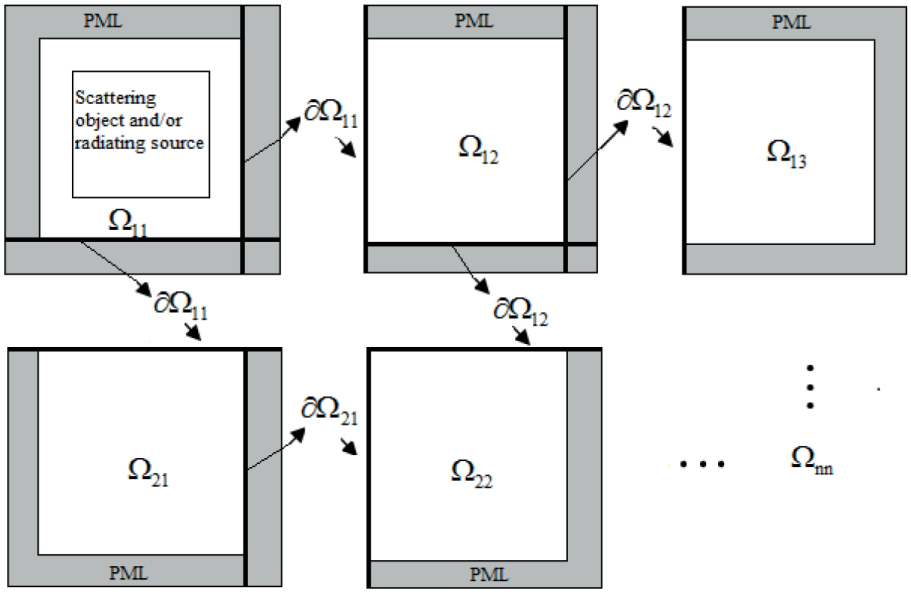

Figure 4. Partitioning a typical 2D electromagnetic scattering and/or radiation problem truncated by PML.

$$\Omega = \bigcup_{i,j} \Omega_{ij}, \text{ and } \Omega_{ij} \bigcap_{ij \neq lm} \Omega_{lm} = \Phi, \tag{13}$$

where $i, j = 1, 2, 3, ..., n$, and $\Omega_{ij} (i, j \neq 1)$ stand for free space only. Then, after solving the field over Ω_{11}, the solution is permanently stored (on hard disk) and the memory is cleared. Next, the field is solved over Ω_{12}, and the process is repeated until Ω_{nn}. Here it is important to point that on the exterior boundaries of PML in $\Omega_{12} u = 0$, whereas the left-hand vertical boundary $\partial\Omega_{12}$ is borrowed from $\partial\Omega_{11}$. In addition, as the upper and lower PML parts of Ω_{12} form continuation to the PML in Ω_{11}, (9) has to be satisfied in these parts. In conclusion, this implies that once a subdomain is solved, any adjacent subdomain can be considered without restriction on sequency. Interestingly, this method requires not to solve for all the domain Ω if one is interested in fields at specific locations far from the source and/or scatterer. That is, only the adjacent subdomains that lead to the location under interest need to be solved.

Details smaller than the cell size can be lost when quantization of space of finite size is applied. This is a known drawback of the FDTD method [13]. To overcome this drawback, subgridding techniques have been introduced in the literature [24–33]. In such techniques, part of the FDTD grid is replaced with a finer grid, which is called the subgrid [13]. Then the fields on the boundary of one grid are imposed on the boundary of the finer grid. This is to attract the reader's attention in order not to be confused with the presented technique in this work as the concept of subgridding may lead to confusion. More precisely, subgridding in this study refers to domain decomposition, and the reader may refer to [34,35] for other decomposition techniques for even more complicated problems. However, in this study the author focuses on the SEM performance when domain decomposition is involved.

4. Results

Two electromagnetic problems are studied for the purpose of demonstrating the presented decomposition technique. One is scattering type and the other is radiating type. The utilized numerical method in this study is SEM, which is known for its high accuracy [11,33,36–41]. It is important to note that the proposed technique is not restricted to SEM as the finite difference method (FDM) or FEM can also be utilized.

In the case of SEM, Gauss–Legendre–Lobatto (GLL) grids are applied with Legendre polynomials being the test functions. The PML region is discretized into rectangular elements so that each element has an aspect ratio close to unity in order to reduce the deterioration in the accuracy due to elemental deformation [38]. For GLL grids, the optimum values of the attenuation factor α recommended in [11] are utilized in this work. The spatial discretization in terms of SEM of the governing differential equations using the continuous Galerkin method is introduced by Mahariq et al. in [39]. In the case of the discontinuous Galerkin method, Riemann solvers can be utilized in order to match the solution at the interfaces between elements [41].

4.1. Scattering

Scattering from a loss-free dielectric cylinder excited by a perpendicularly incident plane wave is chosen first for demonstration. In micro-scale, i.e. when the radius of the dielectric cylinder is several times the wavelength of the illuminating plane wave, the scattered field is focused behind the cylinder, producing the so-called photonic nano-jet [39,42,43]. Under some special cases where a long photonic nano-jet [42] is expected, the unbounded medium (or free space), where the cylinder is embedded, has to be truncated by the PML in such a way that the required solution can be obtained. Hence, large computational domains may be encountered.

In Figure 5, the magnitude of the total (incident-scattered) electric field ($|E_z^{inc} + E_z^{scat}|$) is shown for an illuminating plane wave of the form $E_z^{inc} = \exp(-jkx)$ (TEz polarization is considered), when the diameter and the refractive index of the dielectric cylinder are taken as 7λ and 1.3, respectively. Here the dimensions of the problem are normalized with respect to the wavelength λ, with $\lambda = 1$.

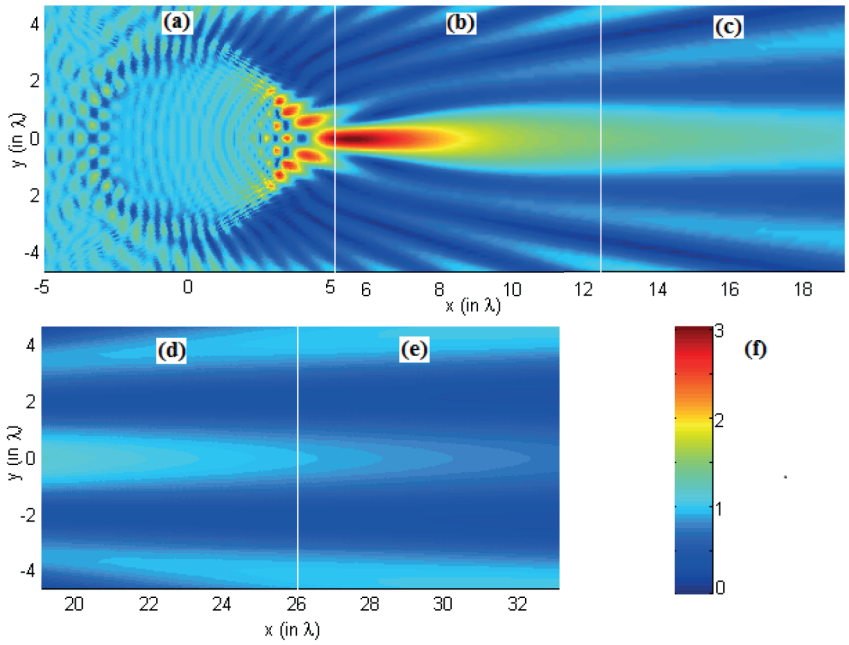

Figure 5. The magnitude of the total (incident-scattered) electric field, ($|E_z^{inc} + E_z^{scat}|$) inside and outside a dielectric cylinder of 7λ in diameter and of 1.3 refractive index. The region of interest is partitioned into 5 adjacent subdomains represented by (a), (b), (c), (d), (e), and (f) represents the color mapping of field magnitude.

Considering the complexity in the codes applying the SEM, the available computational resources can solve with difficulty the scattered field from a cylinder of 9λ in diameter mainly due to the size of the resulting linear system of equations. By using the proposed technique in the current study, the field is solved first within and near the scatterer (dielectric cylinder) as shown in Figure 5a. Then the solution is permanently stored and the memory is cleared and prepared for a new computation as mentioned in Section 3. After that, depending on the region of interest, the adjacent subdomain that leads to the interest can be solved. For the example chosen here, the subdomain represented by Figure 5b is then considered, but one cannot solve the field in Figure 5c before 5b as no information is provided about the boundary conditions. It is important to note that Figure 5d is the adjacent solution for that shown in Figure 5c.

4.2. Radiation

Radiation from a line source located along the z-axis is solved over a relatively large region in terms of the wavelength λ. The radiation of the line source is governed by (again, TEz polarization is considered)

$$\nabla^2 u + k^2 u = -\delta(r), \tag{14}$$

where r denotes the radial distance from the origin, and the solution is given in terms of Hankel function of the second kind of order zero as $u(r) = (j/4)H_0^{()}(k|r|)$. To avoid the singularity in the solution, the free-space

region is truncated around the source as shown in Figure 6, and the exact solution is imposed on the boundary $\partial\Omega_{in}$. Therefore, the subdomain Ω_{11}, which is bounded by $\partial\Omega_{in}$ and the PML, has to be solved first.

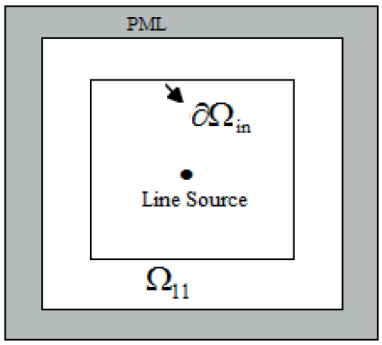

Figure 6. The definition of the radiating line source problem.

By applying the proposed technique, the solution is obtained by SEM over the region of interest Ω that covers a square area of $180\lambda \times 180\lambda$. The real part of the radiated electric field in a portion of Ω is shown in Figure 7, where the white lines represent the boundaries of the subdomains forming the presented portion of Ω. It is important to note that each subdomain Ω_{ij} has an area of $10\lambda \times 10\lambda$; hence, 324 subdomains have to be solved in order to cover Ω. As seen from Figure 7, the solution is continuous and looks as if it is obtained over Ω in one computation. As the exact solution to this problem is available, the relative error defined in (8) is calculated in each subdomain and is averaged over all. The averaged relative error over Ω is 0.0012. For engineers, this error is very satisfactory when compared with that obtained by the finite difference or the low-order finite element method. However, in terms of the accuracy of SEM, this error seems relatively large when compared with that obtained from the 1D problem introduced in Section 2. This does not originate from the proposed solution technique when applied in 2D, but it is due to the limitation in the application of PML. That is, when the incident angle θ, which is the angle between the normal to PML and the incident plane wave, tends to 90°, the wave is not successfully attenuated in the PML [4,11]. This situation occurs in the very far subdomains that are either along the x-axis or y-axis. However, as the near-field and far-field zones are defined in terms of the size of the radiator (hence, in terms of the wavelength), the distance considered in this example is relatively large.

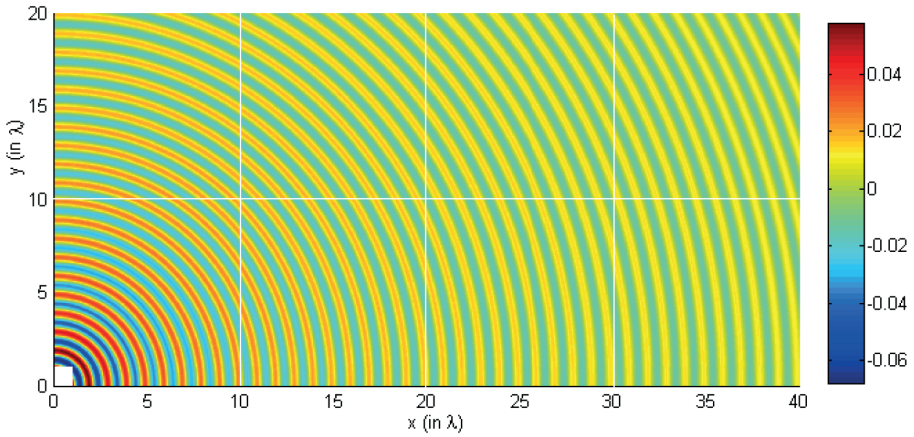

Figure 7. The real part of the radiated electric field from a line source positioned at the origin as obtained by SEM in a portion of Ω. The white lines represent the boundaries of the corresponding subdomains.

It is worth estimating the total number of unknowns that are required to resolve the electric field within Ω. If 50 nodes are assumed to resolve one wavelength (in the case of FDM or FEM), then the total number of nodes will be approximately 81 million, where the nodes simulating the field in the PML are excluded. Computationally speaking, such a number of unknowns is extremely large and requires much larger memory than a typical PC has. However, with the aid of the solution technique introduced in the current study, the solution is obtained using a moderate PC and even without applying any of the parallelization techniques.

5. Conclusion

In this paper, a domain decomposition technique utilizing the mathematical consequences to the introduction of PML has been presented and verified by SEM for the first time in order to successfully solve electromagnetic fields in scattering and radiation problems. Numerical demonstrations either in 1D or 2D reveal that very large problems can be handled by using this technique and show that near and far electromagnetic fields can be solved after customizing the problem to the available computational resources. In terms of the PML formulation introduced in this work, the technique is well explained and presented in such a way that other numerical methods such as finite difference or finite element methods can be utilized to approximate the governing partial differential equations.

As demonstrated in this work, the line source problem shows that the SEM can be applied with domain decomposition to solve far fields from a radiator in a domain involving millions of unknowns with typical engineering accuracy. When this technique is extended to 3D problems, several hundreds of billions of unknowns can be tackled. There are two limitations restricting the maximum number of unknowns in this technique. One arises from the nature of the PML. The second is that this method of solution requires the existence of no obstacles in the free-space region surrounding the antenna or the scatterer. The latter could be overcome by sweeping techniques.

Acknowledgment

The author acknowledges the partial support from the Scientific and Technological Research Council of Turkey.

References

[1] Paris T, Hurd FK. Basic Electromagnetic Theory. 2nd ed. New York, NY, USA: McGraw-Hill, 1969.

[2] Sadiku O, Matthew N. Numerical Techniques in Electromagnetics. 2nd ed. Boca Raton, FL, USA: CRC Press, 2000.

[3] Mittra R. A look at some challenging problems in computational electromagnetics. IEEE Antenn Propag M 2004; 46: 18-32.

[4] Kuzuoglu M, Mittra R. A systematic study of perfectly matched absorbers. In: Werner DH, Mittra R, editors. Frontiers in Elecromagnetics. 2nd ed. Piscataway, NJ, USA: IEEE Press, 2000.

[5] Ergül Ö, Gürel L. Efficient parallelization of the multilevel fast multipole algorithm for the solution of large-scale scattering problems. IEEE T Antenn Propag 2008; 56: 2335-2345.

[6] Ergül Ö, Gürel L. Rigorous solutions of electromagnetic problems involving hundreds of millions of unknowns. IEEE Antenn Propag M 2011; 53: 18-27.

[7] Ergül Ö, Gürel L. Fast and accurate analysis of large-scale composite structures with the parallel multilevel fast multipole algorithm. J Opt Soc Am A 2013; 30: 509.

[8] Laurence H, Trefethen L. Wide-angle one-way wave equations. J Acoust Soc Am 1988; 84: 1397-1404.

[9] Bérenger J. A perfectly matched layer for the absorption of electromagnetic waves. J Comput Phys 1994; 114: 185-200.

[10] Berenger JP. A historical review of the absorbing boundary conditions for electromagnetics. Forum for Electromagnetic Research Methods and Application Technologies 2015; 9.

[11] Mahariq I, Kuzuoğlu M, Tarman H. On the attenuation of perfectly matched layer in electromagnetic scattering problems with spectral element method. Appl Comput Electrom 2014; 29: 701-710.

[12] Bucci O. Computational complexity in the solution of large antenna and scattering problems. Radio Sci 2005; 40: 1027-1039.

[13] Taflove A, Hagness S. Computational Electrodynamics: The Finite-Difference Time-Domain Method. 3rd ed. London, United Kingdom: Artech House, 2005.

[14] Liuge D, Rui Z, Qinggong C, Yahai W. A NTFF transformation method in planar near-field antenna measurement derived from FDTD. In: 10th International Symposium on Antennas, Propagation & Electromagnetic Theory (ISAPE) 2012; New York, NY, USA: IEEE. pp. 101-104.

[15] Luebbers R, Kunz S, Schneider M, Hunsberger F. A finite-difference time-domain near zone to far zone transformation. IEEE T Antenn Propag 1991; 39: 846-857.

[16] Bucci O, D'Elia G, Migliore D. An effective near-field far-field transformation from truncated and inaccurate amplitude-only data. IEEE T Antenn Propag 1999; 47: 1377-1385.

[17] Pierri R, D'Elia G, Soldovieri F. A two probes scanning phaseless near-field far-field transformation technique. IEEE T Antenn Propag 1999; 47: 792-802.

[18] Migliore D, Soldovieri F, Pierri R. Far-field antenna pattern estimation from near-field data using a low-cost amplitude-only measurement setup," IEEE T Instrum Meas 2000; 49: 71-76.

[19] Xu L, Hagness C, Choi K, Daniel W. Numerical and experimental investigation of an ultrawideband ridged pyramidal horn antennas with curved launching plane for pulse radiation. IEEE Antenn Wirel Pr 2003; 2: 505-509.

[20] Zhou B, Wang S, Yu W. An efficient approach to predict far field pattern in FDTD simulation. IEEE Antenn Wirel Pr 2004; 3: 148-151.

[21] Çapoğlu R, Taflove A, Backman V. A frequency-domain near-field-to-far-field transform for planar layered media. IEEE T Antenn Propag 2012; 60: 1878-1885.

[22] Sacks S, Kingsland M, Lee R, Lee F. A perfectly matched anisotropic absorber for use as an absorbing boundary condition. IEEE T Antenn Propag 1995; 43: 1460-1463.

[23] Werner H, Mittra R. New field scaling interpretation of Berenger's PML and its comparison to other PML formulations. Microw Opt Techn Let 1997; 16: 103-106.

[24] Kim S, Hoeffer J. A local mesh refinement algorithm for the time-domain finite-difference method using Maxwell's curl equations. IEEE T Microw Theory 1990; 38: 812-815.

[25] Zivanovic S, Yee K, Mei K. A subgriding method for the time-domain finite-difference method to solve Maxwell's equations. IEEE T Microw Theory 1991; 39: 471-479.

[26] Prescott T, Shuley V. A method for incorporating different sized cells into the finite-difference time-domain analysis technique. IEEE Microw Guided W 1992; 2: 434-436.

[27] El-Raouf H, EI-Diwani E, Ammar A, EI-Hefnawi F. A FDTD hybrid M3d 24-Yee scheme with subgridding for solving large electromagnetic problems. Appl Comput Electrom 2002; 17: 23-29.

[28] Bérenger J. A huygens subgridding for the FDTD method. IEEE T Antenn Propag 2006; 54: 3797-3804.

[29] Pernice W, Payne F, Gallagher D. Simulation of metallic anostructures by using a hybrid FDTD-ADI subgridding method. In: Proceedings of International Conference of Electromagnetics in Advanced Applications; July 2007. New York, NY, USA: IEEE. pp. 633-635.

[30] Kopecký R, Persson M. Subgridding method for FDTD modeling in the inner ear. In: Proceedings of the International Society for Optical Engineering; April 2004. SPIE. pp. 398-401.

[31] Abaenkovs M, Costen F, Bérenger J, Himeno R, Fujii M. Huygens subgridding for 3-D frequency-dependent finite-difference time-domain method. IEEE T Antenn Propag 2012; 60.9: 4336-4344.

[32] Ramli1 KN, Abd-Alhameed A, See H, Excell S, Noras M. Hybrid computational scheme for antenna-human body interaction. Prog Electromagn Res 2013; 133: 117-136.

[33] Mehdizadeh O, Paraschivoiu M. Investigation of a two-dimensional spectral element method for Helmholtz's equation. J Comput Phys 2003; 189: 111-129.

[34] Engquist B, Ying L. Sweeping preconditioner for the Helmholtz equation: moving perfectly matched layers. Multiscale Model. Multiscale Model Sim 2011; 9: 686-710.

[35] Tsuji P, Engquist B, Ying L. A sweeping preconditioner for time-harmonic Maxwell's equations with finite elements. J Comput Phys 2012; 231: 3770-3783.

[36] Lee J, Liu Q. A 3-D spectral-element time-domain method for electromagnetic simulation. IEEE T Microw Theory 2007; 55: 983-991.

[37] Lee J, Xiao T, Liu Q. A 3-D spectral-element method using mixed-order curl conforming vector basis functions for electromagnetic fields. IEEE T Microw Theory 2006; 54: 437-444.

[38] Mahariq I, Tarman H, Kuzuoğlu M. On the accuracy of spectral element method in electromagnetic scattering problems. Inter J Comp Theory Eng 2014; 6: 495-499.

[39] Mahariq I, Kurt H, Tarman H, Kuzuoğlu M. Photonic nanojet analysis by spectral element method. IEEE Phot J 2014; 6.5: 1-14.

[40] Mahariq I, Kurt H, Kuzuoğlu M. Questioning degree of accuracy offered by the spectral element method in computational electromagnetics. Appl Comput Electrom 2015; 30: 698-705.

[41] Lee J, Chen J, Liu Q. A 3-D discontinuous spectral element time-domain method for Maxwell's equations. IEEE T Antenn Propag 2009; 57: 2666-2674.

[42] Kim M, Scharf T, Mühlig S, Rockstuhl C, Herzig P. Engineering photonic nanojets. Opt Express 2011; 19: 10206-10220.

[43] Gu G, Zhou R, Chen Z, Xu H, Cai G, Cai Z, Hong M. Super-long photonic nanojet generated from liquid-filled hollow microcylinder. Opt Lett 2015; 40: 625-628.